JOURNAL OF CATALYSIS 58, 303–312 (1979)

On the Kinetics and Mechanism of the CO Oxidation over Polycrystalline Iridium

T. MATSUSHIMA,[1] M. HASHIMOTO, AND I. TOYOSHIMA

The Research Institute for Catalysis, Hokkaido University, Sapporo 060, Japan

Received October 20, 1978; revised January 15, 1979

The kinetics of the CO oxidation was studied over polycrystalline iridium under ultrahigh vacuum conditions. The reaction was first-order in CO and zero-order in O_2 for low CO pressures, while it was inhibited by CO above a certain critical CO pressure. Above that pressure the reaction was first-order in O_2 and negative-order in CO. The amount of adsorbed CO and oxygen during the catalyzed reaction was determined with flash-desorption, AES, and UPS. Above the critical CO pressure the amount of adsorbed CO was equal to that in the CO/Ir equilibrium (nonworking) system. It decreased sharply around the CO pressure and was very small at lower pressures. The amount of adsorbed oxygen decreased smoothly as the CO pressure increased and became very small around the critical CO pressure. This kinetic behavior can be explained in terms of a Langmuir–Hinshelwood mechanism and a change in the rate-limiting process.

INTRODUCTION

Several kinetic studies on the CO oxidation over iridium have recently appeared in the literature (*1–6*). Christmann and Ertl (*1*) have studied the temperature dependence of the steady-state CO_2 production rate over an Ir(110) single crystal surface, which is very similar to that obtained over various palladium and platinum single crystal surfaces. They have concluded that CO_2 is formed through an Eley–Rideal process (ER), namely, CO (gas or phys. ads.) + O (chem. ads.) $\rightarrow CO_2$. Küppers and Plagge (*2*) have studied the same reaction over an Ir(111) surface and obtained a similar temperature dependence, which has been explained in terms of the ER mechanism. When the surface covered by both CO and oxygen is heated, however, they have observed that CO_2 is produced through a Langmuir–Hinshelwood process (LH), namely, CO (chem. ads.) + O (chem. ads.) $\rightarrow CO_2$. Weinberg and his co-workers (*5*, *6*) have explained the temperature dependence of the steady-state CO_2 production rate in terms of the LH mechanism, considering the changes with the temperature in the concentrations of CO(a) and oxygen on the surface during the catalyzed reaction. On the other hand, recent molecular beam (*7*, *8*) and transient isotope tracer (*9*, *11*) methods have provided ample evidence that on Pt and Pd surfaces CO_2 is produced merely through the LH process. In addition, the reaction mechanism at a steady-state on those metals has been analyzed at a level of the rates of the elementary processes (*12–14*). There is a sharp change in the rate-limiting process of the steady-state CO_2 production which occurs at a certain critical temperature and pressure of the reactants (*12–14*). A similar

[1] To whom all correspondence should be sent.

0021-9517/79/080303-10$02.00/0

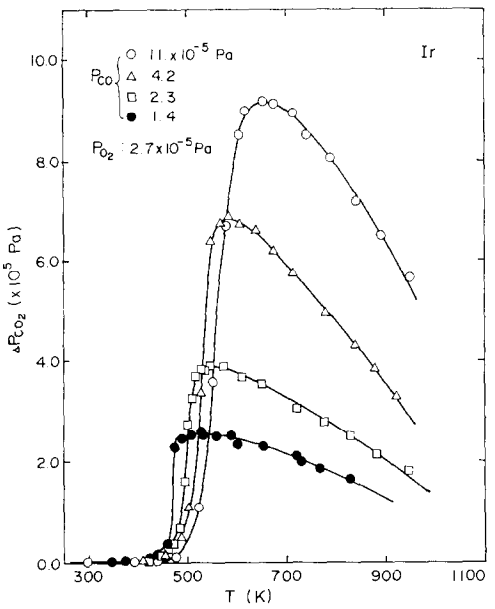

FIG. 1. Variation of the rate of CO_2 production at a steady-state with temperature at various fixed pressures of CO and O_2.

change is expected on Ir since the metal has a catalytic activity to this oxidation as high as Pt and Pd, and the kinetic behavior reported so far (*1–6*) is quite similar to that on these metals. In the case of Ir, however, neither the kinetics nor the mechanism at a steady-state have been analyzed in detail.

In this paper the detailed kinetic studies at a steady-state under low pressures and also the amount of adsorption of CO and oxygen during the catalyzed reaction are reported. The results are explained in terms of the Langmuir–Hinshelwood mechanism and a change in the rate-limiting process.

EXPERIMENTAL

The experimental apparatus and procedures for kinetic studies were essentially the same as those reported previously (*9–11, 14*). The system was a bakable ultrahigh vacuum apparatus with a base pressure of less than 3×10^{-7} Pa(1 Pa = 7.5×10^{-3} Torr). A polycrystalline Ir foil ($30 \times 6 \times 0.05$ mm) was used as a catalyst. The sample was mounted between two 0.3-mm-diameter tungsten wires by spot-welding, which were also spot-welded to thick molybdenum rods which served as current leads for resistive heating. The temperature was monitored with a Pt–Pt/Rh thermocouple spot-welded on the foil. Prior to the experiments the sample was exposed to 1×10^{-4} Pa of oxygen at 1500°K for several hours, and flashed to 1700°K for a few tens of minutes. Several repetitions of this treatment were sufficient to establish stable catalyst behavior, such as the highest activity for the CO oxidation and the stable adsorption–desorption phenomena of CO and oxygen. The above oxygen treatment was applied even in a series of measurements whenever the stable catalyst behavior was not observed. An iridium foil pretreated in a way similar to that mentioned above was analyzed by AES in a separate system. The surface was clean except for a trace of silicon.

AES and UPS studies were conducted, separately from the above kinetic studies, with a Vacuum Generators ESCA-3 Spectrometer, which had Ar^+ bombardment, AES, UPS, and residual gas analysis capabilities. The base pressure in the instrument was about 1×10^{-8} Pa. The system included a sample preparation chamber and a separate spectrometer chamber in which the electron energy analyzer was located. Reactant gases were admitted through leak valves in the preparation chamber. The Ir foil was mounted on the end of the rotatable cylindrical probe which was spot-welded to a nickel plate mechanically clamped. The temperature reading by a chromel-alumel thermocouple embedded in the end of the probe was calibrated by another thermocouple which was spot-welded directly on the back of the Ir foil. The total pressure was monitored by an ionization gauge in the spectrometer chamber. The gauge was located near the diffusion pump. So another gauge was inserted near the catalyst in the spectrometer chamber, the

difference in the reading between the above two gauges was determined, and then the pressure near the catalyst during the measurements was estimated. The composition of gases admitted was analyzed by a mass spectrometer in the preparation chamber. For adsorption studies at low temperatures, the sample was cooled by flowing liquid nitrogen via the cooling pipe embedded in the probe. The Ir foil was cleaned by repeated cycles of heating for several hours at 900°K in 1×10^{-4} Pa of oxygen followed by Ar^+ bombardment until a clean surface was obtained as judged by AES. In these cleaning procedures the Ar^+ bombardment was needed because the sample could be heated only up to 900°K.

RESULTS

1. *Kinetic Studies*

The CO_2 production rate at a steady-state was studied as a function of the catalyst temperature and the partial pressures

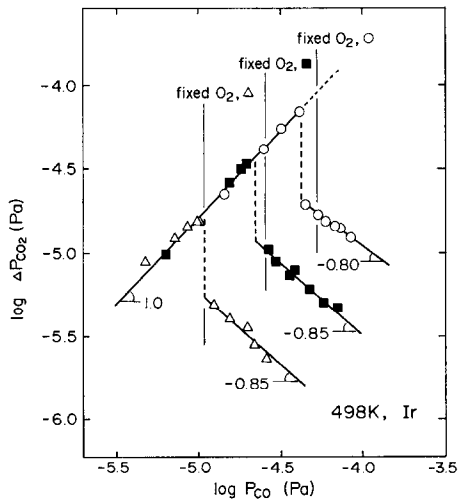

FIG. 2. Variation of the rate of CO_2 production with CO pressure at 498°K and various fixed O_2 pressures. The vertical solid bars indicate fixed O_2 pressures: △, 1.1×10^{-5} Pa; ■, 2.7×10^{-5} Pa; and ○, 5.3×10^{-5} Pa. The reaction orders are indicated along the linear portion of each curve. The vertical dotted lines show sharp drops in the CO_2 production.

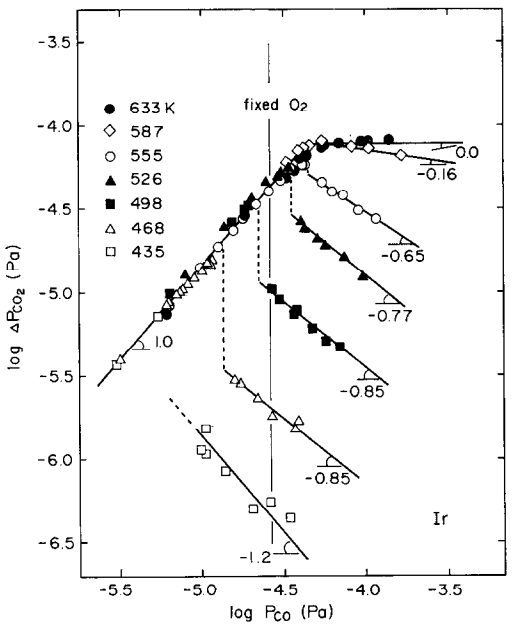

FIG. 3. Variation of the rate of CO_2 production with CO pressure at various temperatures under a fixed O_2 pressure of 2.7×10^{-5} Pa. There are sharp transitions in the rate law at some critical CO pressures drawn by vertical dotted lines.

of the reactants. The observed $m/e = 44$ mass signal was proportional to the CO_2 production rate since the reaction system was pumped continuously. It is assumed that CO_2 interacts so weakly with Ir surface that the partial pressure exerts no influence on the oxidation rate, since CO_2 is not adsorbed at the temperatures studied here as shown in Section 2b.

1a. Temperature dependence. The steady-state oxidation rate depended strongly on the catalyst temperature and showed a maximum around the CO desorption temperature (*1*, *2*, *4*, *5*, *16*, *17*). Some typical results are shown in Fig. 1. The rate increased slightly with an increase in the temperature below a certain value where it grew up sharply to a maximum, and decreased again at higher temperatures. This temperature which showed a sharp increase in the rate shifted to higher values with an increase in the CO pressure. The maximum rate showed first-order de-

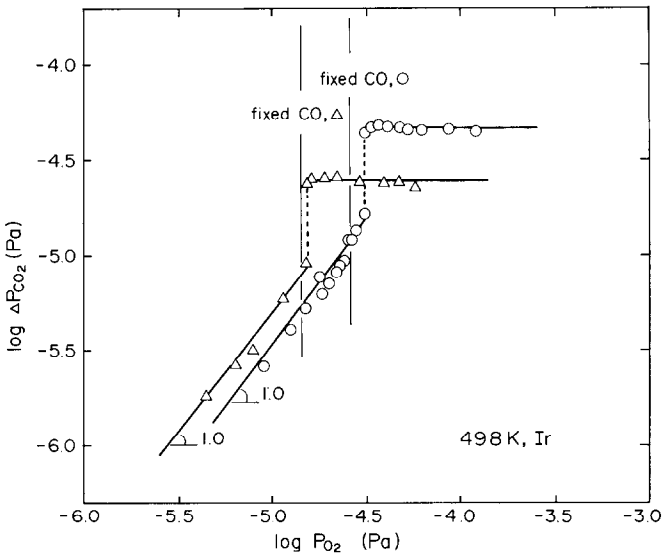

FIG. 4. Variation of the rate of CO_2 production with O_2 pressure under fixed CO pressures: △, 1.4×10^{-5} Pa; and ○, 2.7×10^{-5} Pa. The vertical dotted lines show sharp jumps in the CO_2 production.

pendence to the CO pressure when the pressure was less than twice the O_2 pressure, while above that pressure the maximum rate did not increase with the CO pressure. Figure 1 shows the rate observed under $P_{CO} = 11.1 \times 10^{-5}$ Pa, which gave the same maximum value as that under $P_{CO} = 5.4 \times 10^{-5}$ Pa. The temperature dependence is also seen in Fig. 3, where the same O_2 pressure is used.

1b. Reaction order with respect to CO. Figures 2 and 3 summarize the measured CO_2 production rates at a steady-state as a function of CO pressure for several fixed oxygen pressures and several fixed temperatures. The reaction orders with respect to CO are shown for each linear portion of the figures. The measured rates are independent of the sequence of pressures used. These figures are both characterized by sharp transitions at a certain CO pressure. Below that pressure the reaction was first-order in CO and independent of the temperature while above that pressure it was negative-order and very sensitive to the temperature. The absolute CO_2 production rate in the former region was close to that on Pd (*15*) and Pt (*14*) in similar conditions. The magnitude of the negative-order, which measured the extent of inhibition of the reaction by CO, was large when the catalyst temperature was low. In light of the discussion below, most of this change is due to variation in CO(a) which depends strongly on the temperature. At 633°K there is no longer inhibition in the high-pressure region, rather the zero-order dependence indicates a saturation condition. The rate dropped discontinuously at the critical CO pressure as shown by the vertical dotted lines. Around that pressure it took several tens of minutes to reach a steady-state. It appears that two elementary processes compete with each other to govern a main surface species and the difference between those rates is very slight around the critical CO pressure. The critical pressure shifted toward low values with a decrease of the temperature.

1c. Reaction order with respect to O_2. Holding the CO pressure constant, we determined the order of CO_2 production rate at a steady-state with respect to oxygen. The results are shown in Fig. 4.

Like carbon monoxide the oxygen dependence showed sharp transitions at a certain O_2 pressure. The rate showed first-order and zero-order behavior below and above the transition pressure. The reaction rate below the transition pressure decreased with an increase in the CO pressure, while above that pressure the saturation level increased with the CO pressure. The critical O_2 pressure also shifted to high values with an increase in the CO pressure, as expected from the dependence on the CO pressure.

1d. Amount of CO adsorbed during the catalyzed reaction. To understand the kinetics it is now important to determine the amount of adsorbed CO and oxygen during the catalyzed reaction, especially around the critical ratio of the CO and oxygen partial pressures. The amount of adsorbed CO was first determined in the course of the reaction by means of a flash-desorption technique. Second, UPS was applied to the same subject as mentioned in Section 2c. The flash-desorption technique has been applied to determine the amount of adsorbed CO during the catalyzed reaction on Pd (*18*) and Pt (*14, 19*). The same procedures were used here. The catalyst was heated to 800°K where CO was not adsorbed, from a steady-state working condition at a fixed temperature, while the CO and CO_2 peaks were monitored. The amount of CO adsorbed initially was calculated as the sum of these peak areas. Figure 5 shows the CO adsorption isotherm determined in this way at 468°K with 2.7×10^{-5} Pa of O_2, i.e., working condition, and also without oxygen, i.e., nonworking condition (CO/Ir equilibrium system). The coverage was defined as the sum of CO and CO_2 peak areas relative to the maximum area of the CO peak which was obtained by flashing from room temperature under a steady flow of CO. Above the critical CO pressure drawn by the vertical dotted line, the coverage during the reaction equalled the value measured in the

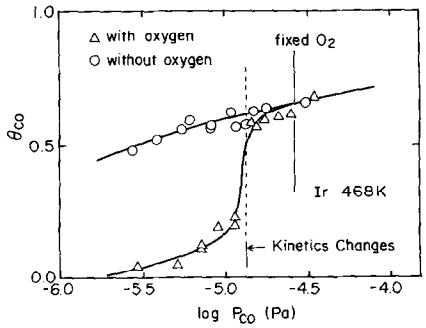

FIG. 5. CO adsorption isotherm determined by flash desorption in the presence and absence of oxygen. The vertical dotted line shows a critical CO pressure.

CO/Ir equilibrium system, i.e., the adsorption–desorption process of CO is in quasi-equilibrium. The CO coverage decreased sharply around the critical CO pressure and became very small under lower pressures. In the latter region, the coverage was much less than that in the CO/Ir equilibrium system, i.e., the CO adsorption process was not in equilibrium. Above that critical pressure the desorption peak area of CO_2 was very small as compared with that of CO and no O_2 was desorbed even the catalyst was flashed to 1400°K. This fact means that the amount of oxygen adsorbed above the critical CO pressure is much less than that of CO.

2. Adsorption Studied with AES and UPS

The adsorption of oxygen and carbon monoxide during the reaction and also the adsorption–desorption of carbon dioxide at low temperatures were studied with AES and UPS.

2a. Oxygen adsorption during the catalyzed reaction. The amount of adsorbed oxygen during the catalyzed reaction was followed by monitoring the peak-to-peak height of the differentiated oxygen Auger signal. The catalyst temperature was maintained at high values to reduce the contribution from oxygen Auger signal due to adsorbed carbon monoxide. The variation of the amount with CO pressure at 643°K is

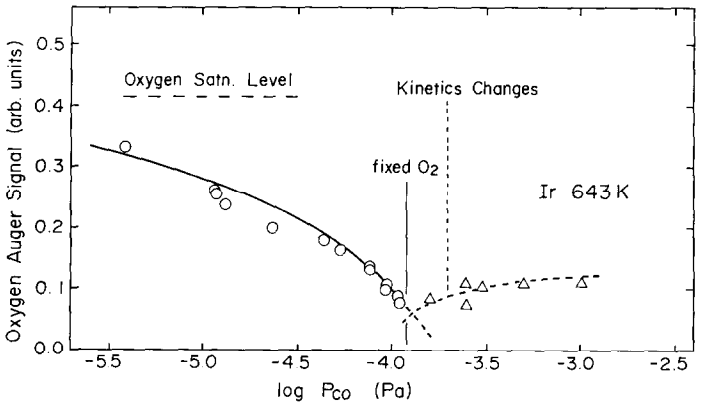

FIG. 6. Steady-state oxygen Auger signal as a function of CO pressure at 643°K and a fixed O_2 pressure of 1.2×10^{-4} Pa. Open circles show oxygen signal not accompanied with a carbon signal. Triangles indicate the presence of a detectable concentration of carbon, probably from adsorbed carbon monoxide.

shown in Fig. 6. The intensity of oxygen signal shown in the figure was normalized to the peak-to-peak height of the iridium Auger signal. Under some conditions a carbon Auger signal was observed indicating chemisorbed carbon monoxide. Those are denoted as triangles in Fig. 6. Except for these points, the oxygen Auger signals contain no contribution from CO(a). Under these experimental conditions all of the adsorbed oxygen was reactive toward CO since the Auger signal vanished when the O_2 supply was terminated. Conclusively, the amount of adsorbed oxygen is significant below the critical CO pressure and very small above the pressure.

2b. Adsorption and desorption of CO_2. CO_2 was adsorbed at 78°K. The clean Ir surface was cooled down to 78°K and exposed to CO_2 at 1×10^{-4} Pa for 300 sec. The photoelectron emission from this surface was analyzed at $h\nu = 40.8$ eV. The results are displayed together with that from the clean surface in Fig. 7. Three new levels appeared which were associated with adsorbed CO_2. The emission from the metal itself was attenuated very much. This may be attributed to the multilayer formation of CO_2 (*20*). A condensed or physisorbed layer of CO_2 on Au (*21*), Ni (*22*), Pt (*23*), and Cu (*24*) has shown a similar spectrum. In those works the level at 8.0 eV is assigned to the $1\pi_g$ orbital, the level at 12.1 eV as the unresolved $1\pi_u$ and $2\sigma_u$, and that at 13.0 eV as the $2\sigma_g$ orbital. The levels in gas phase CO_2 (*25*) are indicated in Fig. 7 (ii) with $2\sigma_u$ level shifted to coincide with the 12.1 eV line. The photoelectron spectrum due to CO_2 adsorbed was not observed after the catalyst was heated to 123°K for 10 min. The desorption temperature of adsorbed CO_2 is lower than that temperature. A similar result has been observed on Pt (*23*). Thus desorption of CO_2 will be a rapid process under all experimental conditions used here for kinetic studies. Once this molecule is formed by the oxidation of CO on the surface it will be immediately released into the gas phase. Therefore it is reasonable to assume that the CO_2 partial pressure has no effect on the oxidation rate.

2c. CO adsorption studies with UPS. UPS can be easily used to monitor the variation of the amount of adsorbed CO during the catalyzed reaction since the photoelectron emission yield from CO molecule is large and the helium resonance light does not decompose adsorbed CO molecules. The photoelectron emission was observed at $h\nu = 40.8$ eV while the clean surface

was exposed to CO of 1×10^{-5} Pa at 465°K. Adsorption of CO leads to the formation of extra peaks at 8.4 and 10.9 eV and a small shoulder around 7.0 eV below the Fermi level. The spectrum is in agreement with that observed from CO on Ir(111) (*2*, *26*), (100) (*27*), and polycrystalline (*26*) surfaces. The electron energy levels in gas phase CO (*25*) are drawn by vertical lines in Fig. 7 (iii) with 4σ level shifted to coincide with 10.9 eV line. The levels at 7.0, 8.4, and 10.9 eV are assigned to 5σ, 1π, and 4σ orbitals, respectively (*26*, *27*).

In order to know the variation of the amount of adsorbed CO during the catalyzed reaction, the peak area due to $(5\sigma + 1\pi)$ orbital was plotted against the CO pressure. The results are shown in Fig. 8. The upper panel shows two spectra obtained under different working conditions, which are very close to the critical CO pressure. The peak due to $(5\sigma + 1\pi)$ orbital is cross-hatched. The lower panel shows the variation of the peak area with CO pressures at a fixed O_2 pressure. Those are drawn as triangles. Open circles show the peak area of the same orbital in the absence of O_2. The amount of adsorbed CO increased sharply around 2×10^{-5} Pa of CO and became equal to that in the CO/Ir nonworking (equilibrium) condition at higher CO pressures. This result confirms the CO adsorption isotherm during the reaction determined by flash desorption.

As summaries, the reaction kinetics changes discontinuously at a certain critical CO pressure which increases with increasing O_2 pressure and the temperature. Below that CO pressure, the oxygen adatom is predominant on the surface, whereas above that pressure the surface is mainly covered by CO. Those kinetic and adsorption phenomena are quite similar to those on Pd (*13*, *15*, *18*) and Pt (*12*, *14*, *19*, *28*).

DISCUSSION

In this section we will discuss mainly the relationship between the rate-limiting pro-

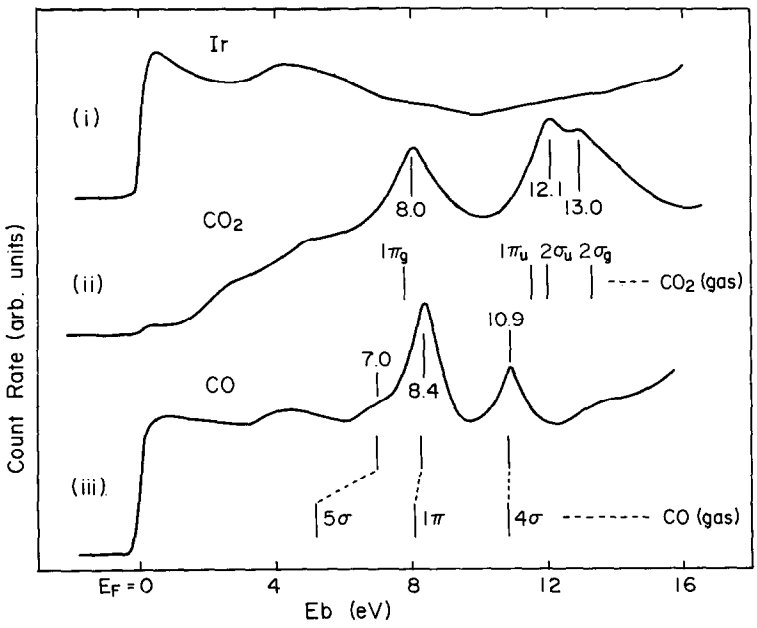

FIG. 7. Photoelectron spectra of (i) a clean Ir surface at 465°K, (ii) a condensed film of CO_2 at 78°K, and (iii) a CO adlayer at 465°K. The peak positions in the spectra of gaseous CO_2 and CO are also drawn by vertical solid lines.

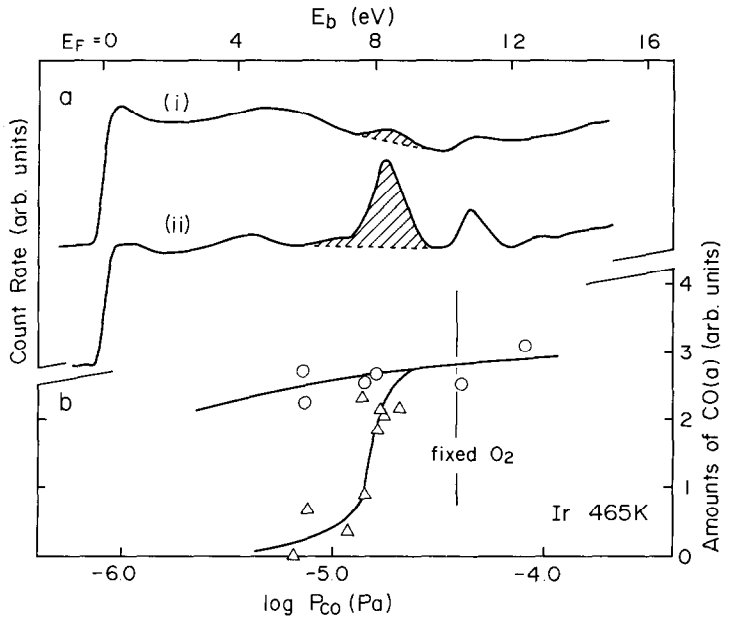

FIG. 8. (a) Photoelectron spectra from Ir surface during the catalyzed reaction. The steady state pressures (in Pa) of CO and O_2 are in the form (P_{CO}, P_{O_2}): (i) 1.45×10^{-5}, 4.8×10^{-5}; and (ii) 1.7×10^{-5}, 4.8×10^{-5}. (b) The amount of adsorbed CO determined by UPS in the absence (○) and presence (△) of oxygen. It is shown as relative peak area of ($5\sigma + 1\pi$) orbital of CO(a).

cess, the kinetics of the overall CO oxidation at a steady-state, and the amount of absorbed CO and oxygen during the catalyzed reaction. Only a qualitative discussion is given here since in a previous publication on Pt (*14*), which is very similar, we have presented a detailed description of the reaction mechanism.

1. Temperature Dependence

The temperature dependence of the rate shown in Fig. 1 is in general agreement with that reported on single crystal (110) (*1*) and (111) (*2*, *4*) Ir surfaces. The effect of the CO pressure on the dependence is quite similar to that on Pt when the CO pressure is less than the O_2 pressure (*14*). Below the temperature where the rate was maximized, the apparent activation energies were estimated to be 130–80 kJ/mol, which were close to the desorption energy of adsorbed CO, ~120 kJ/mol (*1*, *2*, *4*). From this comparison Ertl *et al.* (*1*, *2*) have concluded that the CO desorption is the rate-limiting process. According to the recent kinetic analysis of the LH process (*5*, *6*, *29*), however, this process is faster than the thermal desorption of adsorbed CO at relatively low temperatures if the oxygen coverage is significant. In other words CO(a) is removed as CO_2 through the LH process rather than the thermal desorption. Therefore the latter cannot control the removal rate of adsorbed CO in the course of the reaction where the oxygen pressure is significant. The same conclusion has been derived on Pt (*12*, *14*) and Pd (*18*, *30*). As discussed below the dissociative adsorption of oxygen is rate-limiting in this temperature region which corresponds to CO pressures above the critical value. The adsorption–desorption process of CO is in quasi-equilibrium. The adsorption rate of oxygen is determined by the O_2 collision frequency and the surface area available for

O_2 adsorption. This area depends strongly on the amount of adsorbed CO since CO(a) prevents oxygen from being adsorbed. Thus the area should increase with the temperature, being due to the decrease of CO(a). At higher temperatures and when the CO pressure is less than the critical value at temperatures as high as 555°K ($P_{CO}/P_{O_2} \simeq 2$) (see Fig. 3), the rate is in general limited by the CO adsorption and the decrease of the rate is attributed to the decrease in the CO(a) and O(a)coverage through the thermal desorption or the diffusion into the metal bulk (*31*, *32*). When the CO pressure is higher than twice the O_2 pressure, the rate of the CO_2 production is always limited by the O_2 adsorption regardless of the temperature.

2. *Kinetics and Mechanism*

Sharp transitions in the rate law summarized in Figs. 2, 3, and 4 strongly suggest that a change in the rate-limiting process occurs around the critical CO pressure. The CO adsorption data of Figs. 5 and 8, and also oxygen adsorption data of Fig. 6, facilitate understanding the kinetic behavior of the overall CO_2 production rate. At CO pressures below the critical value CO(a) was not accumulated up to the equilibrium level. This fact means that the removal process of adsorbed CO, i.e., the LH process plus the CO thermal desorption, is faster than the thermal desorption at the equilibrium coverage, i.e., the desorption rate of CO(a) when the adsorption–desorption process of CO is in equilibrium. And further the fact that the amount of CO(a) is much less than the equilibrium value means that the LH process plays a major role in eliminating CO(a) from the surface. In fact, at relatively low temperatures (lower than ~500°K) adsorbed CO is removed as CO_2 through the LH process rather than CO (*29*). The amount of adsorbed oxygen is significant and the surface is deficient in CO(a). The rate-limiting process is the CO adsorption on the oxygen-covered surface. Thus the reaction is first-order in CO, zero-order in O_2 and independent of the temperature. The amount of adsorbed oxygen decreased smoothly as the CO pressure increased and became very small around the critical CO pressure. The thermal desorption rate of adsorbed oxygen is pretty small at the temperatures studied here (*31*, *32*). At a steady-state the adsorption rate should be equal to the removal rate of adsorbed oxygen which is the CO_2 production rate. Below the critical CO pressure, the CO_2 production increases with an increase in the CO pressure and then the adsorption rate of oxygen should also increase. Therefore the surface is uncovered to a larger extent with an increase in the CO pressure to offer adsorption sites for oxygen adsorption and then the oxygen adatom which is predominant on the surface decreases, as is actually seen in Fig. 6. On the other hand above the critical CO pressure the amount of adsorbed CO was almost equal to that observed in the CO/Ir equilibrium (nonworking) system. The amount of adsorbed oxygen is much smaller than that of CO(a), implying that the oxygen adsorption is slower than the consumption rate of O(a) by the reaction with CO(a). Hence adsorbed oxygen cannot be accumulated on the surface and the oxygen adsorption is the rate-limiting process of the CO_2 production. Thus the reaction should be first-order in O_2. The oxygen adsorption is severely retarded by CO(a) and the amount of CO(a) increases with a decrease of the temperature. So the magnitude of the negative-order should increase with a decrease of the temperature, as is actually seen in Fig. 3.

3. *CO Inhibition Region*

The inhibition region by CO(a), i.e., CO pressures above the critical value or O_2 pressures below the critical value, is extended as the temperature decreases.

Quite similar phenomena were observed on Pt and explained quantitatively in terms of the LH process (*14*). Qualitatively the LH process eliminating CO(a) from the surface has a significant activation energy (~40 kJ mol^{-1}) (*2*, *5*, *6*), while the adsorption of CO needs little activation energy (*4*, *16*, *17*, *27*). At temperatures as high as 555°K where the LH process is very fast (*5*, *6*), the boundary between the inhibition and noninhibition regions is determined by the balance between the supply rates of oxygen and carbon monoxide onto the surface (*14*). In the case of Ir, the ratio of the CO pressure to the O_2 pressure was obtained to be 2 at the critical pressure and such high temperatures. At lower temperatures it is determined by the comparison of the rate of the LH process with the adsorption rate of CO. So the critical CO pressure should shift to low values from the critical value at temperatures higher than 555°K, i.e., $P_{CO}/P_{O_2} = 2$ with a decrease of the temperature as was actually observed.

ACKNOWLEDGMENTS

This work was supported in part by the Matsunaga Science Foundation, and also a Grant-in-Aid for Scientific Research from the Ministry of Education, No. 343001.

REFERENCES

1. Christmann, K., and Ertl, G., *Z. Naturforsch.* **28a**, 1144 (1973).
2. Küppers, J., and Plagge, A., *J. Vac. Sci. Technol.* **13**, 259 (1976).
3. Falconer, J. L., Wentrcek, P. R., and Wise, H., *J. Catal.* **45**, 248 (1976).
4. Hagen, D. I., Nieuwenhuys, B. E., Rovida, G., and Somorjai, G. A., *Surface Sci.* **57**, 632 (1976).
5. Ivanov, V. P., Boreskov, G. K., Savchenko, V. I., Egelhoff, W. F., Jr., and Weinberg, W. H., *J. Catal.* **48**, 269 (1977).
6. Zhdan, P. A., Boreskov, G. K., Egelhoff, W. F., Jr., and Weinberg, W. H., *Surface Sci.* **61**, 377 (1976).
7. Engel, T., and Ertl, G., *Proc. 7th Int. Vac. Congr. and 3rd Int. Conf. Solid Surfaces*, (*Vienna*, 1977) p. 1365.
8. Engel, T., and Ertl, G., *Chem. Phys. Lett.* **54**, 95 (1978).
9. Matsushima, T., *Shokubai* (*Catalyst*) **20**, 140P (1978) (in Japanese).
10. Matsushima, T., *J. Catal.* **55**, 337 (1978).
11. Matsushima, T., *Surface Sci.* **79**, 63 (1979).
12. Matsushima, T., Almy, D. B., and White, J. M., *Surface Sci.* **67**, 89 (1977).
13. Matsushima, T., and White, J. M., *Surface Sci.* **67**, 122 (1977).
14. Matsushima, T., *Bull. Chem. Soc. Japan* **51**, 1956 (1978).
15. Matsushima, T., Almy, D. B., Foyt, D. C., Close, J. S., and White, J. M., *J. Catal.* **39**, 277 (1975).
16. Comrie, C. M., and Weinberg, W. H., *J. Chem. Phys.* **64**, 250 (1976).
17. Nieuwenhuys, B. E., and Somorjai, G. A., *Surface Sci.* **72**, 8 (1978).
18. Matsushima, T., Mussett, C. J., and White, J. M., *J. Catal.* **41**, 397 (1976).
19. Golchet, A., and White, J. M., *J. Catal.* **53**, 266 (1978).
20. Norton, P. R., Tapping, R. L., Broida, H. P., Gadzuk, J. W., and Waclawski, B. J., *Chem. Phys. Lett.* **53**, 465 (1978).
21. Atkinson, S. J., Brundle, C. R., and Roberts, M. W., *Faraday Discuss. Chem. Soc.* **58**, 62 (1974).
22. Brundle, C. R., and Carley, A. F., *Faraday Discuss. Chem. Soc.* **60**, 51 (1975).
23. Norton, P. R., and Richards, P. J., *Surface Sci.* **49**, 567 (1975).
24. Norton, P. R., and Tapping, R. L., *Chem. Phys. Lett.* **38**, 207 (1976).
25. Turner, D. W., Baker, C., Baker, A. D., and Brundle, C. R., "Molecular Photoelectron Spectroscopy." Interscience, New York, 1970.
26. Zhdan, P. A., Boreskov, G. K., Boronin, A. I., Schepelin, A. P., Egelhoff, W. F., Jr., and Weinberg, W. H., *Surface Sci.* **71**, 267 (1978).
27. Broden, G., and Rhodin, T. N., *Solid State Commun.* **18**, 105 (1976).
28. Bonzel, H. P., and Ku, R., *J. Vac. Sci. Technol.* **9**, 663 (1972).
29. Matsushima, T., unpublished data.
30. Matsushima, T., and White, J. M., *J. Catal.* **40**, 334 (1975).
31. Zhdan, P. A., Boreskov, G. K., Boronin, A. I., Egelhoff, W. F., Jr., and Weinberg, W. H., *Surface Sci.* **61**, 25 (1976).
32. Ivanov, V. P., Boreskov, G. K., Savchenko, V. I., Egelhoff, W. F., Jr., and Weinberg, W. H., *Surface Sci.* **61**, 207 (1976).